Paper 21

PARTLY-GROOVED, EXTERNALLY-PRESSURIZED BEARINGS

By G. G. Hirs*

In externally-pressurized bearings, forces can be transmitted by means of a fluid film interposed between the two bearing surfaces by an external source. In the conventional types, the equilibrium of external forces and fluid film forces becomes stable by making the fluid flow through external restrictions before entering the clearance space.

In the new types, external restrictions are superfluous. Stability and load capacity are ensured by directing the flow in the clearance space, by means of recurrent grooves on one of the two bearing surfaces, towards a zone where both surfaces are plain.

INTRODUCTION

EXTERNALLY-PRESSURIZED BEARINGS incorporate external restrictions in order that the equilibrium of external forces and fluid film forces remains stable. In Fig. 21.1, a journal bearing with one row of external restrictions around the circumference is depicted. In Fig. 21.2, an end bearing suitable for axial loads is shown; the bearing incorporates one central external restriction. The directions of the fluid flow are also shown in the figures. The flow can be seen to be subjected to two passages in series, the first passage being determined by the external restriction, and the second by the thickness of the lubricant film near the restriction. Then, pressures downstream of a restriction will tend to increase if the local film thickness decreases, and vice versa. This phenomenon is shown in Fig. 21.2, by comparing the pressure distribution for a small and great film thickness; the fluid film below the journal can be seen to behave as a spring. This property is a prerequisite to the stability of external forces and fluid film forces in equilibrium.

Adams (1)† and Mannan *et al.* (2) describe externally-pressurized journal bearings in which the external restrictions were eliminated—see Figs 21.3 and 21.4, respectively. Although the authors do not mention it, thrust bearings can be redesigned analogously—see Figs 21.5 and 21.6, respectively. The bearings of Figs 21.3–21.7 have one feature in common with the bearings incorporating external restrictions—a fluid flow is subjected to different passages connected in series. However, all passages are determined by film thicknesses in the present case, which is in contrast to the conventional types of Figs 21.1 and 21.2. By comparing the pressure distribution at a small and a great film thickness in Fig. 21.5, it can be seen that the lubricant film in these new types also behaves as a spring. However, the stiffness of the lubricant film is attributed to differences in the height of the pressure distribution for the two positions in the bearing of Fig. 21.2, whereas the stiffness of the lubricant film is attributed

The MS. of this paper was received at the Institution on 22nd November 1965.

* *Research Engineer, Institute T.N.O. for Mechanical Constructions, Delft, Holland.*

† *References are given in Appendix 21.IV.*

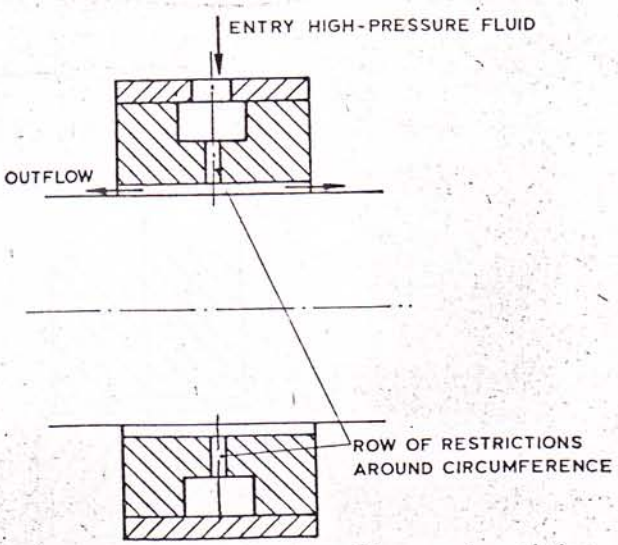

Fig. 21.1. Journal bearing with external restrictions

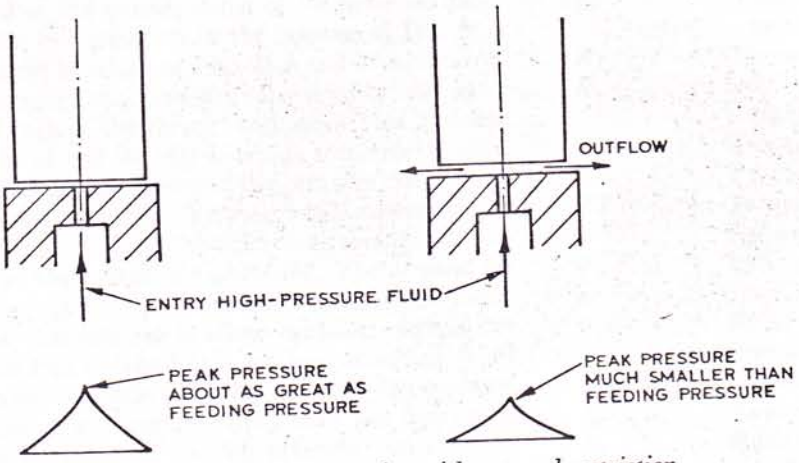

Fig. 21.2. Thrust bearing with external restriction

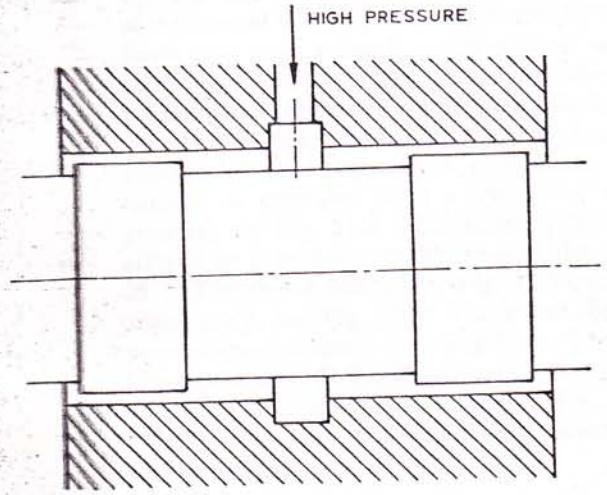

Fig. 21.3. Step journal bearing

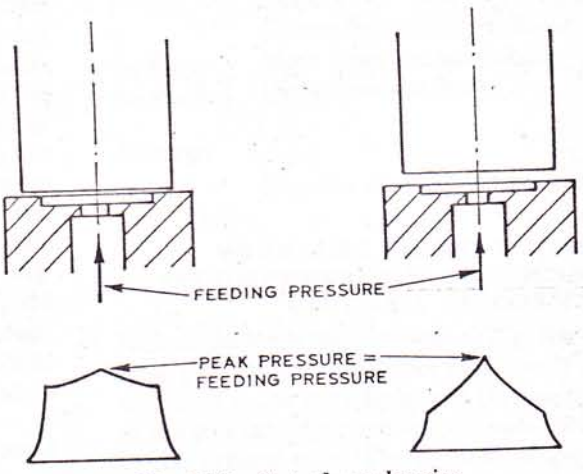

Fig. 21.5. Step thrust bearing

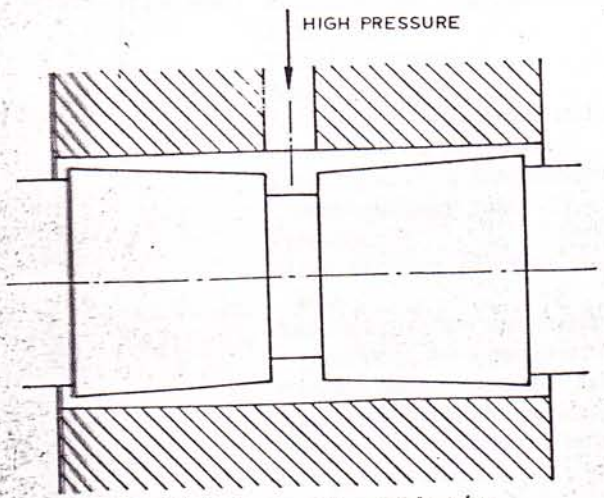

Fig. 21.4. Tapered journal bearing

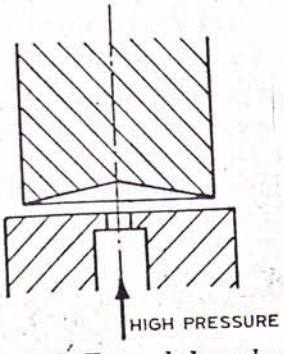

Fig. 21.6. Tapered thrust bearing

to differences in the overall shape of the pressure distribution for the two positions in the bearing of Fig. 21.5.

In the journal bearings of Figs 21.3 and 21.4, the conditions governing the pressure distribution are more complicated than in the thrust bearings of Figs 21.5 and 21.6, as soon as the journal bearings run eccentrically. Then the rotational symmetry of the pressure distribution vanishes. It has to vanish, because radial forces can be counteracted only if pressure differences around the circumference of the journal are generated. The demand for rotationally asymmetric pressure build-up in journal bearings implies that journal bearings without external restrictions, see Figs 21.3 and 21.4, are less promising. They can be expected to obtain a smaller load-carrying capacity, and a greater power consumption, than the bearing of Fig. 21.1 at an identical feeding pressure and identical radial clearance, width, and diameter. This drawback arises from the need for greater clearances than the radial clearance h_0 over part of the bearing surfaces in Figs 21.3 and 21.4. Pressure differences around the circumference of the journal will be greatly suppressed by short-circuiting flows over such areas. It seems obvious now that short-circuiting flows in these journal bearings need to be counteracted. Only one method is available: a decrease in the passages to circumferential flow without affecting the passages to axial flow. Thus, part of one of the bearing surfaces is provided with a pattern of recurrent axial grooves; see Fig. 21.7. This journal bearing may be considered as a further development of the bearing of Fig. 21.3. The thrust bearing of Fig. 21.5 can be redesigned analogously, see Fig. 21.8. The radial grooves will suppress tangential short-circuiting flows. Then, the grooved bearings of Fig. 21.8 will counteract skewing forces more effectively than the thrust bearing of Fig. 21.5.

In the following, attention will in particular be devoted to grooved journal bearings.

Notation

F	Dimensionless restriction.
$H\ (= h/h_0)$	Dimensionless film thickness.
h	Film thickness.
h_0	Radial clearance.
l	Axial co-ordinate.
l_0	Axial length of a grooved and a plain zone.
P	Dimensionless pressure.
P_1	Load capacity in dimensionless form for the incompressible case.
p	Pressure.
p_m	Mean pressure per unit projected bearing area.
p_0, p_1	Ambient pressure and feeding pressure, respectively, for a compressible lubricant.
Δp	Pressure difference across axial length l_0 for an incompressible lubricant.
Q	Energy consumption per unit time.
q	Energy consumption per unit area and unit time.
q_m	Mean energy consumption per unit area and unit time.
R	Gas constant.
R_1	Load capacity in dimensionless form for the compressible case.
r	Radius.
T	Temperature.
ΔT	Temperature difference.
γ	Ratio of groove width to wavelength.
δ	Ratio of the film thicknesses in a groove and on a dam, journal and bearing concentric.
ϵ	Ratio of eccentricity and radial clearance.
η	Dynamic viscosity.
$\lambda\ (= l/r)$	Axial co-ordinate in dimensionless form.
λ_0	Ratio of the length l_0 to the radius.
λ_1	Ratio of the length of the plain zone and the radius.
λ_2	Ratio of the length of the grooved zone and the radius.
ρ	Density.
φ	Circumferential co-ordinate.
$\phi_l, \phi_{\varphi r}$	Mass flows per unit width.
$\phi_\lambda, \phi_\varphi, \phi_t$	Dimensionless flows.

Subscript

m	Denotes an averaged quantity.

PRESSURE BUILD-UP FOR AN INCOMPRESSIBLE LUBRICANT AND A UNIFORM VISCOSITY

In two previous publications (3) (4) the bearing surfaces were provided with grooves for reasons other than those discussed in the introduction to this paper. The derivation of the pressure distribution proceeds along identical lines in the present case. The number of grooves around the circumference is assumed to be very great. Fig. 21.9 depicts an eccentric cross-section of the bearing. If both surfaces are plain, the film thickness can be represented by

$$h = h_0(1+\epsilon \cos \varphi)$$

If grooves are present on one of the surfaces, their depths have to be superimposed upon

$$h_0(1+\epsilon \cos \varphi)$$

If, for instance, grooves with a rectangular cross-section are cut into one of the surfaces, the film thickness can either be represented by

$$h = h_0(1+\epsilon \cos \varphi) \quad \text{or} \quad h = h_0(\delta+\epsilon \cos \varphi)$$

The parameter δ gives the ratio of the film thicknesses in a groove and on a dam, when journal and bearing are concentric with respect to one another.

The two general expressions for the mass flows in a lubricant film can now be represented:

$$\phi_l = \frac{-\rho}{12\eta}\frac{\partial p}{\partial l}h^3 \quad . \quad . \quad . \quad (21.1)$$

$$\phi_{\varphi r} = \frac{-\rho}{12\eta r}\frac{\partial p}{\partial \varphi}h^3 \quad . \quad . \quad . \quad (21.2)$$

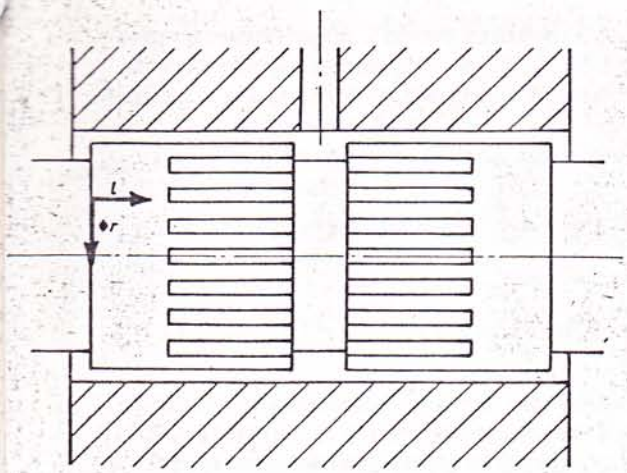

Fig. 21.7. Partly-grooved journal bearing

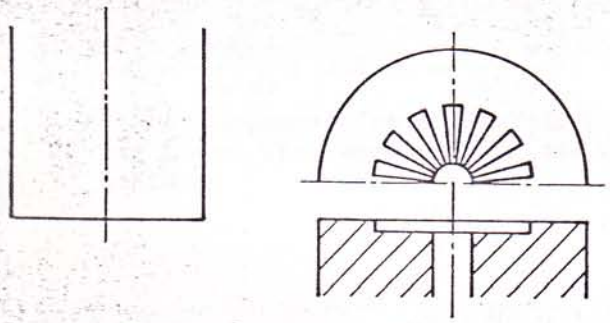

Fig. 21.8. Radially-grooved thrust bearing

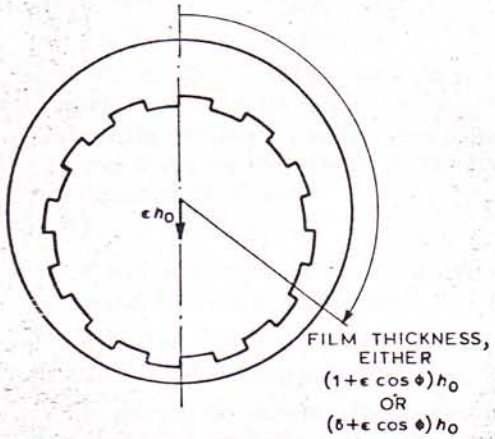

Fig. 21.9. Cross-section journal bearing

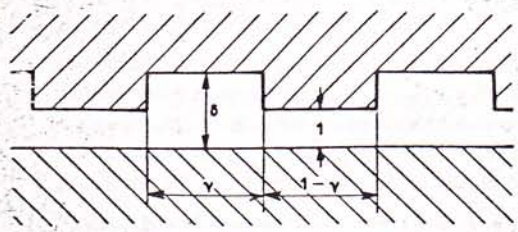

Fig. 21.10. Groove and dam

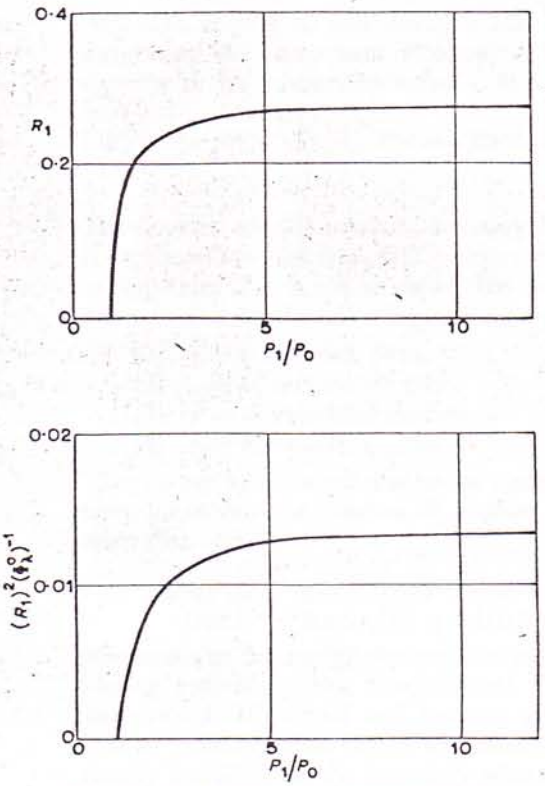

Fig. 21.11. Influence of compressibility

in which the co-ordinate l represents the axial direction and the co-ordinate φ the circumferential direction; see Fig. 21.7. The two equations can be derived from the Navier–Stokes equations by imposing the usual assumptions of lubrication analysis. Equations (21.1) and (21.2) do not demand that the film thickness be specified. However, some general properties of pressure and flow can be noted which are attributable to the wave-like character of the film thickness. Pressure and flow can thus be expected to incorporate a wave-like component but these wave-like components are not of direct interest to present knowledge of these bearings.

Therefore, equations (21.1) and (21.2) will be stripped of all wave-like components. The assumption that the number of grooves be very great simplifies this procedure. It can be carried out whilst assuming the co-ordinate φ to be almost constant. It also means that the gradient, $\partial p/\partial l$, density ρ, and flow $\phi_{\varphi r}$ can be regarded as uniform when travelling in the direction φ across a wavelength. Then, equation (21.1) can be subjected to a connection in parallel, and equation (21.2) to a connection in series.

It follows that

$$(\phi_l)_m = \frac{-\rho}{12\eta}\frac{\partial p}{\partial l}(h^3)_m \quad . \quad . \quad . \quad (21.3)$$

$$\phi_{\varphi r} = \frac{-\rho}{12\eta}\left(\frac{\partial p}{r\,\partial \varphi}\right)_m \frac{1}{(1/h^3)_m} \quad . \quad (21.4)$$

in which the subscript m indicates the quantities averaged

over one wavelength. The two equations clearly show that all wave-like quantities are now extinct, and that different passages are attached to the grooved surface for the two directions of pressure flow.

The two passages are defined for a groove of rectangular cross-section:

$$(h^3)_m = \{(1-\gamma)(1+\epsilon\cos\varphi)^3+\gamma(\delta+\epsilon\cos\varphi)^3\}h_0{}^3 \quad . \quad . \quad . \quad (21.5)$$

$$\frac{1}{(1/h^3)_m} = \frac{h_0{}^3}{[(1-\gamma)/(1+\epsilon\cos\varphi)^3]+[\gamma/(\delta+\epsilon\cos\varphi)^3]} \quad . \quad . \quad . \quad (21.6)$$

in which the parameter γ denotes the width of the groove with respect to that of the wavelength; see Fig. 21.10.

It is convenient to make use of dimensionless quantities in the mathematical treatment:

$$\lambda = \frac{l}{r}; \quad P = \frac{p}{\Delta p}; \quad H = \frac{h}{h_0};$$

$$\phi_\lambda = \frac{12(\phi_l)_m\eta r}{\rho h_0{}^3\,\Delta p}; \quad \text{and} \quad \phi_\varphi = \frac{12\phi_{\varphi r}\eta r}{\rho h_0{}^3\,\Delta p}$$

where Δp indicates the excess pressure in the central feeding groove. Then, equations (21.3) and (21.4) can be rewritten:

$$\phi_\lambda = -\frac{\partial P}{\partial\lambda}(H^3)_m \quad . \quad . \quad . \quad (21.7)$$

$$\phi_\varphi = -\frac{\partial P}{\partial\varphi}\frac{1}{(1/H^3)_m} \quad . \quad . \quad . \quad (21.8)$$

The continuity condition demands that

$$\frac{\partial\phi_\lambda}{\partial\lambda}+\frac{\partial\phi_\varphi}{\partial\varphi} = 0 \quad . \quad . \quad . \quad (21.9)$$

Equations (21.7), (21.8), and (21.9) give the pressure distribution over the whole bearing area. For the zone where the two bearing surfaces are plain, parameter $\delta = 1$ or $\gamma = 0$ require to be inserted. The boundary conditions to equation (21.9) are:

$P = 0$ at $\lambda = 0$;

P and ϕ_λ continuous at $\lambda = \lambda_1$, where the plain zone passes into the grooved zone;

and $P = 1$ at $\lambda = \lambda_1+\lambda_2$, indicating that $p = \Delta p$ in the central feeding groove*.

In solving the pressure distribution in journal bearings, perturbation methods with respect to eccentricity have been shown to give reliable results. Therefore, a series expansion for dimensionless pressure P is introduced:

$$P = (P^\circ)_{\epsilon\to 0}+\epsilon(P')_{\epsilon\to 0}+\epsilon^2(P'')_{\epsilon\to 0}+\cdots \quad (21.10)$$

in which the superscripts indicate the number of differentiations with respect to eccentricity ϵ before asserting that eccentricity ϵ vanishes. The treatment is now confined to the components P° and P'—see Appendix 21.I. The resultant of the pressures due to the first-order perturbation with respect to eccentricity ϵ can be obtained by integrating the component $P'\cos\varphi$; it will be directly opposite to the eccentricity vector ϵ. It follows that:

$$P_1 = \frac{1}{\lambda_1+\lambda_2}\int_0^\pi\int_0^{\lambda_1+\lambda_2} P'\cos\varphi\,d\varphi\,d\lambda = \left(\frac{p_m}{\epsilon\,\Delta p}\right)_{\epsilon\to 0} \quad . \quad . \quad . \quad (21.11)$$

The dimensionless number P_1, denoting the load capacity, is expressed as a function of the parameters γ, δ, λ_0, and λ_1 in Appendix 21.I. It can be shown that the number P_1 reduces to zero for the following limiting conditions:

(1) $\lambda_1 = 0$, no plain zone.
(2) $\lambda_2 = 0$, no grooved zone.
(3) $\gamma = 0$, vanishing grooves.
(4) $\delta = 1$, vanishing grooves.

Thus, it can be expected that sets of optimum parameters exist for which the number P_1 obtains extreme values other than zero.

ENERGY CONSUMPTION FOR AN INCOMPRESSIBLE LUBRICANT

For assessing the energy consumption per unit area of the mating surfaces q, the dimensionless flow ϕ_λ must be determined. If journal and bearing are concentric, it follows from equation (21.7), by making use of the continuity condition at the boundary where the plain zone passes into the grooved zone, that

$$\phi_\lambda{}^\circ = -\left(\frac{(H^3)_m}{\lambda_1(H^3)_m+\lambda_2}\right)_{\epsilon\to 0} \quad . \quad (21.12)$$

in which the flow $\phi_\lambda{}^\circ$ can be regarded as the first component of a series expansion of the flow ϕ_λ analogous to equation (21.10).

By definition:

$$\phi_\lambda{}^\circ = \frac{12(\phi_l)_{m,\,\epsilon\to 0}\eta r}{\rho h_0{}^3\,\Delta p} \quad . \quad . \quad (21.13)$$

The average energy consumption per unit area of the mating surfaces is expressed by

$$q = -\frac{\Delta p}{l_0}\frac{(\phi_l)_{m,\,\epsilon\to 0}}{\rho}$$

Eliminating the axial flow $(\phi_l)_{m,\,\epsilon\to 0}$ from the above two identities:

$$\phi_\lambda{}^\circ = -\frac{12q\eta r l_0}{\Delta p^2\,h_0{}^3}$$

A somewhat simpler expression can be derived if the total energy consumption $Q = 2\pi r\,2l_0 q$ is inserted:

$$\phi_\lambda{}^\circ = -\frac{3}{\pi}\frac{Q\eta}{\Delta p^2\,h_0{}^3} \quad . \quad . \quad (21.14)$$

And thus the dimensionless flow $\phi_\lambda{}^\circ$ shows how it depends on the energy consumption.

OPTIMIZING BEARING PARAMETERS FOR AN INCOMPRESSIBLE LUBRICANT

Formulae, whose extreme values had to be determined, have been programmed for a digital computer and, next, they have been subjected to an optimization process. In

* *Other boundary conditions at $\lambda = 0$ and $\lambda = \lambda_1+\lambda_2$ are feasible, as long as the dimensionless pressure in the feeding groove ($\lambda = \lambda_1+\lambda_2$) exceeds the dimensionless ambient pressure ($\lambda = 0$) by unity.*

e process, a continuous non-linear function of up to six dependent variables could be minimized by a refined adient technique; see Dickinson (6).

The three quantities, whose extreme values will be pro-ded, are:

(1) The load capacity as a result of a first-order pertur-tion with respect to eccentricity is given in dimensionless rm in equation (21.11). By looking for maximum values the ratio $p_m/\Delta p$ at several values for the length–radius tio λ_0, the feeding pressure will contribute as much as ossible to the load capacity and to the stiffness of the earing.

(2) A different criterion evolves by demanding that a reat load capacity should be obtained at a small energy onsumption. This criterion can be expressed by eliminat-ng the feeding pressure Δp from equations (21.11) and 21.14).

It follows that

$$\frac{p_m{}^2 h_0{}^3}{\epsilon^2 Q \eta} = -\frac{3}{\pi}(P_1)^2(\phi_\lambda{}^\circ)^{-1} \quad . \quad (21.15)$$

(3) Another criterion evolves by demanding that a reat load capacity should be obtained at a small through-low. The criterion can be expressed by eliminating the eeding pressure Δp from equations (21.11) and (21.13).

It follows that

$$\frac{p_m h_0{}^3}{\epsilon \phi_t \eta} = -\frac{3}{\pi} P_1(\phi_\lambda{}^\circ)^{-1}$$

nd

$$\phi_t = \frac{2\pi r 2(\phi_t)_{m,\epsilon \to 0}}{\rho} \quad . \quad . \quad (21.16)$$

n which ϕ_t denotes the total volume flow over the two halves of the bearing in unit time.

In other words: the three criteria for optimizing demand hat the load capacity shall be as great as possible while keeping either the feeding pressure, or the energy con-sumption, or the through-flow as small as possible.

In this paper, results on the optimization will be given for length–radius ratios $\lambda_0 = l_0/r = 1$, 2, 3, and 4. By maintaining this ratio constant from the outset, three dimensionless variables γ, δ, and λ_1 remain to be opti-mized. The optimization process requires that they be provided with upper and lower limits. The lower limits to the parameters γ and λ are of great importance in this respect. In offering a resistance as great as possible to cir-cumferential flow, the parameter γ tended to become too small for practical purposes, and the parameter δ tended to become rather great. Therefore, the lower limit to para-meter γ has been held at values which could be expected to be adequate in actual applications ($\gamma = 0{\cdot}1$, 0·2, 0·3, and 0·5).

In the optimization process, the parameter γ always reached the imposed lower limit in the long run. The para-meter λ_1 had to be provided with a lower limit when the quantity P_1, equation (21.11), was subjected to the opti-mization process. Otherwise, it would tend to become too small for practical purposes, and the energy consumption would become excessive. The lower limit imposed upon the parameter λ_1 amounted to 0·1 in all optimizations. When optimizing the quantities $(P_1)^2(\phi_\lambda{}^\circ)^{-1}$ and $P_1(\phi_\lambda{}^\circ)^{-1}$, the parameter λ_1 always exceeded this lower limit.

Now that the limiting conditions are known, the results of the optimization process can be discussed. The parameters and the dependent quantities are given in Table 21.1. Equations (21.11), (21.15), and (21.16) explain the dependent quantities in physical terms. Values shown in italic figures indicate that the quantity in question has

Table 21.1. Data for partly-grooved journal bearings using an incompressible lubricant

γ	δ	λ_1	λ_0	P_1	$(P_1)^2(\phi_\lambda{}^\circ)^{-1}$	$P_1(\phi_\lambda{}^\circ)^{-1}$
0·1	4·94	0·100	1·0	*−0·415*	−0·0291	−0·070
0·1	2·37	0·100	1·0	−0·268	−0·0121	−0·045
0·1	3·53	0·216	1·0	−0·325	*−0·0384*	−0·118
0·1	2·89	0·355	1·0	−0·243	−0·0325	*−0·134*
0·2	3·98	0·100	1·0	*−0·390*	−0·0254	−0·065
0·2	2·90	0·207	1·0	−0·306	*−0·0324*	−0·106
0·2	2·37	0·351	1·0	−0·224	−0·0271	*−0·121*
0·3	3·52	0·100	1·0	*−0·374*	−0·0231	−0·062
0·3	2·60	0·201	1·0	−0·294	*−0·0289*	−0·098
0·3	2·12	0·350	1·0	−0·212	−0·0239	*−0·113*
0·4	3·23	0·100	1·0	*−0·361*	−0·0213	−0·059
0·4	2·40	0·197	1·0	−0·284	*−0·0263*	−0·093
0·4	1·94	0·363	1·0	−0·197	−0·0211	*−0·107*
0·5	3·02	0·100	1·0	*−0·350*	−0·0199	−0·057
0·5	2·27	0·193	1·0	−0·275	*−0·0243*	−0·088
0·5	1·84	0·350	1·0	−0·193	−0·0199	*−0·103*
0·1	6·23	0·100	2·0	*−0·448*	−0·0352	−0·079
0·1	3·76	0·384	2·0	−0·311	*−0·0621*	−0·200
0·1	3·02	0·692	2·0	−0·221	−0·0510	*−0·231*
0·2	5·00	0·100	2·0	*−0·425*	−0·0314	−0·074
0·2	3·11	0·363	2·0	−0·294	*−0·0521*	−0·177
0·2	2·48	0·687	2·0	−0·202	−0·0421	*−0·208*
0·3	4·41	0·100	2·0	*−0·409*	−0·0288	−0·070
0·3	2·79	0·350	2·0	−0·281	*−0·0457*	−0·163
0·3	2·21	0·688	2·0	−0·189	−0·0365	*−0·193*
0·5	3·79	0·100	2·0	*−0·383*	−0·0248	−0·065
0·5	2·46	0·328	2·0	−0·261	*−0·0367*	−0·141
0·5	1·92	0·701	2·0	−0·167	−0·0286	*−0·171*
0·1	7·14	0·100	3·0	*−0·455*	−0·0369	−0·081
0·1	4·11	0·481	3·0	−0·297	*−0·0706*	−0·238
0·1	3·20	1·000	3·0	−0·193	−0·0553	*−0·286*
0·2	5·74	0·100	3·0	*−0·434*	−0·0330	−0·076
0·2	3·40	0·449	3·0	−0·281	*−0·0588*	−0·209
0·2	2·62	0·998	3·0	−0·176	−0·0451	*−0·256*
0·3	5·06	0·100	3·0	*−0·418*	−0·0303	−0·072
0·3	3·07	0·423	3·0	−0·270	*−0·0509*	−0·188
0·3	2·34	1·000	3·0	−0·163	−0·0383	*−0·235*
0·5	4·36	0·100	3·0	*−0·390*	−0·0257	−0·066
0·5	2·76	0·377	3·0	−0·252	*−0·0390*	−0·155
0·5	2·02	1·040	3·0	−0·139	−0·0282	*−0·203*
0·1	7·90	0·100	4·0	*−0·455*	−0·0368	−0·081
0·1	4·52	0·515	4·0	−0·286	*−0·0703*	−0·246
0·1	3·39	1·280	4·0	−0·168	−0·0519	*−0·309*
0·2	6·36	0·100	4·0	*−0·435*	−0·0330	−0·076
0·2	3·76	0·471	4·0	−0·274	*−0·0583*	−0·213
0·2	2·78	1·280	4·0	−0·152	−0·0418	*−0·275*
0·3	5·61	0·100	4·0	*−0·419*	−0·0303	−0·072
0·3	3·42	0·434	4·0	−0·264	*−0·0500*	−0·189
0·3	2·48	1·290	4·0	−0·139	−0·0349	*−0·251*
0·5	4·84	0·100	4·0	*−0·389*	−0·0254	−0·065
0·5	3·12	0·363	4·0	−0·250	*−0·0371*	−0·149
0·5	2·14	1·370	4·0	−0·114	−0·0242	*−0·212*

been subjected to the optimization process. Other dependent quantities have been computed using the parameters found in the optimization of this quantity.

The first two cases presented in Table 21.1 show how the quantity P_1 has been optimized for a groove with a lower limit $\gamma = 0{\cdot}1$, and for the step bearing of Fig. 21.3 ($\gamma = 1$). The favourable influence of the grooves in suppressing short-circuiting flows is now evident. By comparing the two quantities P_1, it is seen that the load capacity of the grooved bearing exceeds that of the step bearing by more than 50 per cent at identical feeding pressures. By comparing the two quantities $(P_1)^2(\phi_\lambda{}^\circ)^{-1}$, equation (21.15), it is seen that the energy consumption of the grooved bearing amounts to about 40 per cent of that of the step bearing at an identical load capacity, radial clearance, and viscosity.

Apart from the second row in Table 21.1, all data concern the partly-grooved bearing. It is seen that increasing groove widths go hand in hand with lower extreme values to the three dependent quantities because of decreasing resistances to short-circuiting flows. By comparing the quantities $(P_1)^2(\phi_\lambda{}^\circ)^{-1}$, it can be seen again that the number incorporating the energy consumption will be affected most. It can also be seen that bearings with the greater length–radius ratios suffer more from decreasing resistances to short-circuiting flows than bearings with the smaller length–radius ratios.

PRESSURE BUILD-UP FOR A COMPRESSIBLE LUBRICANT SUCH AS A GAS

Experience with the conventional types of gas-lubricated bearings indicates that the flow may be considered isothermal. Then, equations (21.3) and (21.4) can be made suitable for gas lubrication by inserting

$$\rho = \frac{p}{RT} \quad . \quad . \quad . \quad . \quad (21.17)$$

and assuming the temperature T to be uniform.

The meaning of the quantities P and ϕ, equations (21.3) and (21.4), will now be extended to compressible flow:

$$P = \frac{p^2}{p_1{}^2 - p_0{}^2}; \quad \phi_\lambda = \frac{24(\phi_l)_m \eta r R T}{(p_1{}^2 - p_0{}^2)h_0{}^3}$$

and

$$\phi_\varphi = \frac{24\phi_{\varphi r}\eta r R T}{(p_1{}^2 - p_0{}^2)h_0{}^3}$$

in which p_1 denotes the pressure in the feeding groove, and p_0 is the ambient pressure. The quantities $\lambda = l/r$ and $H = h/h_0$ remain unchanged. Equations (21.7), (21.8), and (21.9) adequately account for the compressible case.

In Appendix 24.I, the first two components of the series expansion of the quantity P, equation (21.10), have been obtained. Thus the pressure build-up for small eccentricities can be expressed by:

$$\frac{p}{(p_1{}^2 - p_0{}^2)^{1/2}} = (P^\circ + \epsilon P' + \cdots)^{1/2}$$

$$= (P^\circ)^{1/2} + \tfrac{1}{2}\epsilon \frac{P'}{(P^\circ)^{1/2}} + \cdots$$

The load capacity, expressed as a resultant of the pressures directly opposite to the eccentricity vector, is now derived:

$$R_1 = \frac{1}{\lambda_1 + \lambda_2} \int_0^{\lambda_1 + \lambda_2} \int_0^{2\pi} \frac{P' \cos\varphi}{(P^\circ)^{1/2}} \, d\varphi \, d\lambda$$

$$= \left(\frac{P_m}{\epsilon (p_1{}^2 - p_0{}^2)^{1/2}} \right)_{\epsilon \to 0} \quad (21.18)$$

The solution to this integral is discussed in Appendix 21.I. The load capacity R_1 evolves as a function of the bearing parameters γ, δ, λ_1 and λ_2 and the new parameter p_1/p_0 representing the ratio of the feeding pressure to the ambient pressure.

It can again be assumed that equation (21.18) is approximately valid up to reasonably great eccentricities.

ENERGY CONSUMPTION FOR A COMPRESSIBLE LUBRICANT

In the preceding a new definition for the dimensionless flow ϕ_λ has been presented. By confining the treatment to concentrical operation, it reads:

$$\phi_\lambda{}^\circ = \frac{24(\phi_l)_{m,\,\epsilon \to 0} \eta r R T}{(p_1{}^2 - p_0{}^2)h_0{}^3} \quad . \quad (21.19)$$

and equation (21.12) shows its dependence on the bearing parameters. The energy consumption per unit area for concentrical operation is expressed by:

$$q = -\left(\frac{dp}{dl} \frac{(\phi_l)_m}{\rho} \right)_{\epsilon \to 0}$$

where pressure p and density ρ are not uniform in the axial direction. Otherwise, the expression for energy consumption q strongly resembles the one for incompressible flow, in that a pressure differential is multiplied by a volume flow per unit width. Using this expression, and equations (21.17) and (21.19), the following expression for the dimensionless flow $\phi_\lambda{}^\circ$ can be built up:

$$\phi_\lambda{}^\circ = -\frac{24 q \eta r}{(p_1{}^2 - p_0{}^2)h_0{}^3} \left(\frac{1}{p} \frac{dp}{dl} \right)^{-1}$$

Thus, the dimensionless flow $\phi_\lambda{}^\circ$ can be expressed in terms of the average energy consumption per unit area q_m, and the ratio of the feeding pressure and the ambient pressure p_1/p_0:

$$\phi_\lambda{}^\circ = -\frac{24 q_m \eta r l_0}{(p_1{}^2 - p_0{}^2)h_0{}^3 \ln (p_1/p_0)}$$

A somewhat simpler expression evolves if the total energy consumption, $Q = 2\pi r 2 l_0 q_m$, is inserted:

$$\phi_\lambda{}^\circ = -\frac{6}{\pi} \frac{Q\eta}{(p_1{}^2 - p_0{}^2)h_0{}^3 \ln (p_1/p_0)} \quad (21.20)$$

OPTIMIZING BEARING PARAMETERS FOR A COMPRESSIBLE LUBRICANT

Two dimensionless quantities, whose extreme values will be provided, are:

(1) The load capacity in dimensionless form is given in equation (21.18). By looking for extreme values of that

number at several values for the length–radius ratio λ_0 and the pressure ratio p_1/p_0, the feeding pressure will contribute as much as possible to the load capacity and to the stiffness of the bearing.

(2) By eliminating the quantity $(p_1^2-p_0^2)$ between equations (21.18) and (21.20), it follows that:

$$\frac{p_m^2 h_0^3 \ln (p_1/p_0)}{\epsilon^2 Q\eta} = -\frac{6}{\pi}(R_1)^2(\phi_\lambda^\circ)^{-1} \quad (21.21)$$

Extreme values of the quantity $(R_1)^2(\phi_\lambda^\circ)^{-1}$ would result in the highest load capacity for given width, diameter, pressure ratio, viscosity, and radial clearance at the lowest energy consumption.

In the present case, the optimization process is not applied. In a preliminary search for extreme values to the two quantities, it could be demonstrated that the related optimum parameters γ, δ, and λ_1 are almost constant throughout the whole range of pressure ratios $p_1/p_0 < 12$ for each length–radius ratio. This feature is demonstrated for a few cases in Appendix 21.II. Thus optimum parameters of the incompressible case remain valid for the compressible case. Therefore the contents of Table 21.1 can be extended to the compressible case by using the optimum parameters and computing the two dependent quantities indicated above, at several values of the pressure ratio. In order to avoid an excessive number of data, the treatment is confined to only one of the lower limits for the parameter γ (= 0·1). The data are given in Table 21.2. (Italic figures denote extreme values of the quantity in question. The other quantity is computed using the optimum parameters.) Fig. 21.11 shows the two quantities dependent on the pressure ratio p_1/p_0 for a given set of groove parameters. It can be seen that the two quantities asymptotically reach maximum values.

Table 21.2. Data for partly-grooved journal bearings using a compressible lubricant

γ	δ	λ_1	λ_0	p_1/p_0	R_1	$(R_1)^2(\phi_\lambda^\circ)^{-1}$
0·1	4·94	0·100	1·0	1·1	*−0·089*	−0·0013
0·1	3·53	0·216	1·0	1·1	−0·070	*−0·0018*
0·1	4·94	0·100	1·0	1·5	*−0·170*	−0·0049
0·1	3·53	0·216	1·0	1·5	−0·135	*−0·0067*
0·1	4·94	0·100	1·0	2·0	*−0·207*	−0·0072
0·1	3·53	0·216	1·0	2·0	−0·166	*−0·0100*
0·1	4·94	0·100	1·0	4·0	*−0·243*	−0·0100
0·1	3·53	0·216	1·0	4·0	−0·198	*−0·0143*
0·1	4·94	0·100	1·0	6·0	*−0·250*	−0·0106
0·1	3·53	0·216	1·0	6·0	−0·205	*−0·0153*
0·1	4·94	0·100	1·0	12·0	*−0·255*	−0·0110
0·1	3·53	0·216	1·0	12·0	−0·209	*−0·0159*
0·1	6·23	0·100	2·0	1·1	*−0·096*	−0·0016
0·1	3·76	0·384	2·0	1·1	−0·067	*−0·0029*
0·1	6·23	0·100	2·0	1·5	*−0·184*	−0·0059
0·1	3·76	0·384	2·0	1·5	−0·129	*−0·0107*
0·1	6·23	0·100	2·0	2·0	*−0·222*	−0·0087
0·1	3·76	0·384	2·0	2·0	−0·158	*−0·0160*
0·1	6·23	0·100	2·0	4·0	*−0·260*	−0·0119
0·1	3·76	0·384	2·0	4·0	−0·188	*−0·0226*
0·1	6·23	0·100	2·0	6·0	*−0·268*	−0·0126
0·1	3·76	0·384	2·0	6·0	−0·194	*−0·0242*
0·1	6·23	0·100	2·0	12·0	*−0·272*	−0·0130
0·1	3·76	0·384	2·0	12·0	−0·198	*−0·0252*
0·1	7·14	0·100	3·0	1·1	*−0·097*	−0·0017
0·1	4·11	0·481	3·0	1·1	−0·064	*−0·0033*
0·1	7·14	0·100	3·0	1·5	*−0·187*	−0·0062
0·1	4·11	0·481	3·0	1·5	−0·123	*−0·0121*
0·1	7·14	0·100	3·0	2·0	*−0·226*	−0·0091
0·1	4·11	0·481	3·0	2·0	−0·150	*−0·0179*
0·1	7·14	0·100	3·0	4·0	*−0·264*	−0·0124
0·1	4·11	0·481	3·0	4·0	−0·177	*−0·0252*
0·1	7·14	0·100	3·0	6·0	*−0·271*	−0·0131
0·1	4·11	0·481	3·0	6·0	−0·183	*−0·0269*
0·1	7·14	0·100	3·0	12·0	*−0·276*	−0·0135
0·1	4·11	0·481	3·0	12·0	−0·187	*−0·0280*
0·1	7·90	0·100	4·0	1·1	*−0·097*	−0·0017
0·1	4·52	0·515	4·0	1·1	−0·061	*−0·0032*
0·1	7·90	0·100	4·0	1·5	*−0·186*	−0·0062
0·1	4·52	0·515	4·0	1·5	−0·118	*−0·0120*
0·1	7·90	0·100	4·0	2·0	*−0·225*	−0·0090
0·1	4·52	0·515	4·0	2·0	−0·143	*−0·0177*
0·1	7·90	0·100	4·0	4·0	*−0·263*	−0·0123
0·1	4·52	0·515	4·0	4·0	−0·169	*−0·0246*
0·1	7·90	0·100	4·0	6·0	*−0·270*	−0·0130
0·1	4·52	0·515	4·0	6·0	−0·175	*−0·0262*
0·1	7·90	0·100	4·0	12·0	*−0·275*	−0·0134
0·1	4·52	0·515	4·0	12·0	−0·178	*−0·0272*

COMPARISON BETWEEN NEW AND CONVENTIONAL EXTERNALLY-PRESSURIZED JOURNAL BEARINGS

This comparison is restricted to the theoretical work contained in the present paper as far as the new bearing type is concerned. Unique properties of the partly-grooved, externally-pressurized bearing as an actual machine element will evolve in a future paper on experiments with and applications of these bearings. Moreover, the comparison is restricted to two properties previously mentioned:

(1) The contribution of the feeding pressure to the load capacity; see equations (21.11) and (21.18) for the incompressible and the compressible case, respectively.

(2) The contribution of the energy input to the load capacity; see equations (21.15) and (21.21), respectively. Data concerning these two properties presented in Tables 21.1 and 21.2 for the new type should be compared with those concerning the conventional bearing type. The source for data concerning the conventional type is Pinkus and Sternlicht (7). The comparison is restricted to laminar feeding (turbulent feeding gives somewhat better results; turbulent flow in the grooves might also be studied).

The comparison is also restricted to journal bearings with one central row of a sufficiently great number of restrictions. For the incompressible case equations 6.13 and 6.28 of Pinkus and Sternlicht (7) can be used in evaluating the quantities P_1 and ϕ_λ°. They are rewritten in Appendix 21.II. The results of the comparison appear in Table 21.3 for a few width–diameter ratios. It is seen that the way in which the feeding pressure contributes to the load capacity (P_1) is similar for the two cases. However, the power input and the through-flow (ϕ_λ°) are much less favourable for the new type of bearing. This can be explained by comparing the greatly different resistances to pressure flow in the two bearing types, Figs 21.1 and 21.7, at identical radial clearances. By combining the two quantities P_1 and ϕ_λ° as

Table 21.3. Comparison between new and conventional bearing types using incompressible lubricants

Type	γ	δ	λ_1	λ_0	F	P_1	$\phi_\lambda{}^\circ$	$(P_1)^2(\phi_\lambda{}^\circ)^{-1}$
Restriction				1·0	1·146	*0·473*	0·534	0·419
				1·0	0·598	0·426	0·374	*0·486*
				2·0	1·440	*0·301*	0·295	0·308
				2·0	0·799	0·277	0·222	*0·346*
				3·0	1·736	*0·190*	0·212	0·170
				3·0	1·003	0·177	0·167	*0·188*
Groove	0·1	4·94	0·100	1·0		*0·415*	5·918	0·029
	0·1	3·53	0·216	1·0		0·325	2·751	*0·038*
	0·1	6·23	0·100	2·0		*0·448*	5·702	0·035
	0·1	3·76	0·384	2·0		0·311	1·558	*0·062*
	0·1	7·14	0·100	3·0		*0·455*	5·610	0·037
	0·1	4·11	0·481	3·0		0·297	1·249	*0·071*

Table 21.4. Comparison between new and conventional bearing types using compressible lubricants

Type	γ	δ	λ_1	p_1/p_0	λ_0	R_1	$\phi_\lambda{}^\circ$	$(R_1)^2(\phi_\lambda{}^\circ)^{-1}$
Restriction				6	0·95	0·33	0·7	*0·150*
Groove	0·1	3·53	0·216	6	1·00	0·21	2·7	*0·015*
Groove	0·1	4·94	0·100	6	1·00	*0·25*	5·9	0·011

in equation (21.15), it can be seen that identical mean pressures, radial clearances, eccentricities, and viscosities for the two bearing types require that the energy consumption for the grooved bearing shall be approximately ten times greater than that for the bearing with external restrictions. The energy consumption can obtain the same order of magnitude for the two cases by adapting the radial clearance. The radial clearance for a grooved bearing should be 2–2·5 times smaller than that for a bearing with external restrictions, if mean pressures, eccentricities (ϵ), viscosities and energy consumptions are equal for the two cases. The radial clearances need to be diminished far less drastically if it is required that the stiffnesses of the lubricant film ($p_m/\epsilon h_0$) be equal for the two cases. For that matter, the radial clearance for a grooved bearing should be 1·5–1·7 times smaller than that for a bearing with external restrictions, if the stiffnesses, viscosities, and energy consumptions are equal for the two cases.

For compressible lubricants the comparison proceeds along identical lines. In this respect, Figs. 6.2 and 6.3 in Pinkus and Sternlicht (7) are extremely useful. Table 21.4 presents the comparison for one value of the width–diameter ratio and for one value of the ratio of the feeding pressure to the ambient pressure.

CONCLUSIONS

The partly-grooved, externally-pressurized journal bearing is promising so far as the contribution of the feeding pressure to the load capacity and the bearing stiffness are concerned. A comparison with bearings incorporating external restrictions shows that the energy consumption tends to be greater in the new type. The use of this bearing in practice now depends on the simple fabrication and the elegant way of taking it up in a design. These points will be discussed in a future paper.

The theory presented in the present paper has been restricted to static behaviour. Sliding and squeezing will be accounted for in future work. If hydrodynamic action also includes sliding and squeezing, grooves might well be inclined with respect to the direction of sliding motion in order to improve load capacity, stiffness, and stability. To this end, the work contained in the present paper and that in reference (4) on self-acting grooved bearings need to be combined and extended. Inclined grooves also present the possibility of exerting a driving action on the rotatable member; see (3).

ACKNOWLEDGEMENTS

The work reported in this paper is part of a research programme on grooved bearings and seals being carried out at the Institute T.N.O. for Mechanical Constructions, Delft, Holland.

The author wishes to thank Professor H. Blok of the Technological University, Delft, for his continuing interest in the subject and also Mr J. P. J. Lamers for mathematical aid.

APPENDIX 21.I

From equations (21.7) and (21.12) the dimensionless pressure gradient $dP^\circ/d\lambda$ can be obtained for a plain as well as a grooved zone. The use of an incompressible lubricant does not demand the specification of boundary conditions to P°.

Table 21.5. Parameters changing stepwise

γ	δ	λ_1	λ_0	p_1/p_0	R_1
0·1	4·36	0·1	1·0	6·0	−0·252
0·1	4·46	0·1	1·0	6·0	−0·253
0·1	4·56	0·1	1·0	6·0	−0·254
0·1	4·66	0·1	1·0	6·0	−0·253
0·1	4·76	0·1	1·0	6·0	−0·253
0·1	4·84	0·1	1·0	6·0	−0·252
0·1	4·94	0·1	1·0	6·0	−0·250
0·1	5·04	0·1	1·0	6·0	−0·248
0·1	7·06	0·1	4·0	6·0	−0·274
0·1	7·16	0·1	4·0	6·0	−0·274
0·1	7·26	0·1	4·0	6·0	−0·275
0·1	7·36	0·1	4·0	6·0	−0·274
0·1	7·46	0·1	4·0	6·0	−0·274
0·1	7·80	0·1	4·0	6·0	−0·271
0·1	7·90	0·1	4·0	6·0	−0·270
0·1	8·00	0·1	4·0	6·0	−0·269

An explicit solution for P' is:

$$P' = (A\,e^{a\lambda} + B\,e^{-a\lambda}) \cos \varphi$$

where A and B are constants, and

$$a = \left\{(H^3)_m \left(\frac{1}{H^3}\right)_m\right\}^{1/2}_{\varepsilon \to 0}$$

The quantity a reduces to unity at the plain zone. Boundary conditions are:

$P' = 0$ at $\lambda = 0$

P' and P'_λ continuous at $\lambda = \lambda_1$

$P' = 0$ at $\lambda = \lambda_1 + \lambda_2$

The bearing is plain for $0 < \lambda < \lambda_1$, and it is grooved for $\lambda_1 < \lambda < (\lambda_1 + \lambda_2)$.

The full solution to P' allows for an integration as in equation (21.11) which ultimately results in:

$$P_1 = -\frac{3(H_3 - H_2)\pi}{2(\lambda_1+\lambda_2)(\lambda_1 H_3 + \lambda_2)} \times \frac{a \sinh a\lambda_2(\cosh \lambda_1 - 1) + \sinh \lambda_1(\cosh a\lambda_2 - 1)}{a \sinh a\lambda_2 \cosh \lambda_1 + (1/H_{13}) \sinh \lambda_1 \cosh a\lambda_2}$$

where

$$H_{2,3} = (H^{2,3})_{m,\,\varepsilon \to 0}$$

$$H_{13} = \left(\frac{1}{H^3}\right)_{m,\,\varepsilon \to 0}$$

Numerical results are shown in Table 21.1.

The full solutions to P' and P° allow for an integration as in equation (21.18). The full solution to P° has not yet been discussed. One boundary condition needs to be specified in order to make the full solution possible:

$$P^\circ = \frac{{p_0}^2}{{p_1}^2 - {p_0}^2} \quad \text{at} \quad \lambda = 0$$

Thus P°, over the plain zone, is given by:

$$P^\circ = \frac{{p_0}^2}{{p_1}^2 - {p_0}^2} + \frac{\lambda H_3}{\lambda_1 H_3 + \lambda_2} \quad (0 < \lambda < \lambda_1)$$

and P°, over the grooved zone, is given by:

$$P^\circ = \frac{{p_0}^2}{{p_1}^2 - {p_0}^2} + \frac{\lambda_1 H_3}{\lambda_1 H_3 + \lambda_2} + \frac{\lambda - \lambda_1}{\lambda_1 H_3 + \lambda_2} \quad (\lambda_1 < \lambda < (\lambda_1 + \lambda_2))$$

The method employed for solving the integral in equation (21.18) reduces to a numerical approximation by means of a nineteenth degree polynomial.

APPENDIX 21.II

In Table 21.5 it is shown that the optimum parameter δ, when searching for an extreme value to quantity R_1, tends to scarcely alter at a substantial influence of compressibility. This property could be found by altering the parameter δ stepwise and computing the related quantity R_1.

Table 21.6. Optimum parameters for incompressible and compressible lubricants and related dependent quantity

γ	δ	λ_1	λ_0	p_1/p_0	R_1	$(R_1)^2(\phi_\lambda{}^\circ)^{-1}$
0·1	3·30	0·207	1·0	6·0	−0·202	−0·0157
0·1	3·53	0·216	1·0	6·0	−0·205	−0·0153
0·1	3·51	0·362	2·0	6·0	−0·192	−0·0249
0·1	3·76	0·384	2·0	6·0	−0·194	−0·0242
0·1	3·82	0·443	3·0	6·0	−0·182	−0·0278
0·1	4·11	0·481	3·0	6·0	−0·183	−0·0269
0·1	4·20	0·460	4·0	6·0	−0·175	−0·0272
0·1	4·52	0·515	4·0	6·0	−0·175	−0·0262

Parameters on even lines from Table 21.1.

In Table 21.6 it is shown that the optimum parameters δ and λ_1, when searching for an extreme value to the quantity $(R_1)^2(\phi_\lambda{}^\circ)^{-1}$, hardly alter at a substantial influence of compressibility. For the few cases indicated in Table 21.6, extreme values to the dependent quantity in question and the optimum parameters have been determined. They have been compared with parameters used in Table 21.2 and the related quantity $(R_1)^2(\phi_\lambda{}^\circ)^{-1}$.

APPENDIX 21.III

Equations 6.13 and 6.28 of Pinkus and Sternlicht (7) are rewritten as follows:

$$\phi_\lambda{}^\circ = -\frac{F}{\lambda_0(1+F)}$$

$$P_1 = -\frac{3\pi}{2} \frac{F(\cosh \lambda_0 - 1)}{\lambda_0(1+F)(\lambda_0 \cosh \lambda_0 + F \sinh \lambda_0)}$$

An extreme value of the quantity P_1 can be obtained by looking for the related optimum parameter F:

$$F_1 = (\lambda_0 \coth \lambda_0)^{1/2}$$

An extreme value of the quantity $(P_1)^2(\phi_\lambda{}^\circ)^{-1}$ can be obtained by looking for the related optimum parameter F:

$$F_2 = \tfrac{1}{4}\{(1 + 8\lambda_0 \coth \lambda_0)^{1/2} - 1\}$$

which is equivalent to an equation in reference (7). The numerical results for three width–diameter ratios appear in Table 21.3.

APPENDIX 21.IV

REFERENCES

(1) ADAMS, C. R. 'High capacity gas step bearings', *Machine Design* 1962 **34** (March, No. 5), 118.

(2) MANNAN, J., FOWLER, J. H. and CARPENTER, A. L. 'Tapered land, hydrostatic journal bearings', Paper 22, *Lubrication and Wear Convention* 1965 (Instn Mech. Engrs, London).

(3) HIRS, G. G. 'Externally-pressurized bearings with inherent friction compensation', *J. appl. Mech., Trans. Am. Soc. mech. Engrs*, Series E, 1965 **32** (No. 5, June), 285.

(4) HIRS, G. G. 'Load capacity and stability characteristics of hydrodynamic grooved journal bearings', *Trans. Am. Soc. lubric. Engrs* 1965 **8** (No. 3, July), 296.

(5) AUSMAN, J. S. 'The finite gas lubricated journal bearing', Paper 22, *Conference on Lubrication and Wear* 1957 (Instn Mech. Engrs, London).

(6) DICKINSON, J. R. 'Computer program for system optimization', *Trans. Engng Inst. Can.* 1958 **2**, 157.

(7) PINKUS, O. and STERNLICHT, B. *Theory of hydrodynamic lubrication* 1961 (McGraw-Hill Book Co. Inc., New York).